



# Two distinct networks for encoding goals and forms of action: An effective connectivity study

Giuseppe Di Cesare<sup>a,b</sup>, Giada Lombardi<sup>b,c</sup>, Peter Zeidman<sup>d</sup>, Burcu A. Urgan<sup>e,f,g</sup>, Alessandra Scutti<sup>b</sup>, Karl J. Friston<sup>d</sup> , and Giacomo Rizzolatti<sup>a,h,1</sup> 

Affiliations are included on p. 6.

Contributed by Giacomo Rizzolatti; received February 9, 2024; accepted May 6, 2024; reviewed by Rainer Goebel, Fabio Sambataro, and Marco Tettamanti

Goal-directed actions are characterized by two main features: the content (i.e., the action goal) and the form, called vitality forms (VF) (i.e., how actions are executed). It is well established that both the action content and the capacity to understand the content of another's action are mediated by a network formed by a set of parietal and frontal brain areas. In contrast, the neural bases of action forms (e.g., gentle or rude actions) have not been characterized. However, there are now studies showing that the observation and execution of actions endowed with VF activate, in addition to the parieto-frontal network, the dorso-central insula (DCI). In the present study, we established—using dynamic causal modeling (DCM)—the direction of information flow during observation and execution of actions endowed with gentle and rude VF in the human brain. Based on previous fMRI studies, the selected nodes for the DCM comprised the posterior superior temporal sulcus (pSTS), the inferior parietal lobule (IPL), the premotor cortex (PM), and the DCI. Bayesian model comparison showed that, during action observation, two streams arose from pSTS: one toward IPL, concerning the action goal, and one toward DCI, concerning the action vitality forms. During action execution, two streams arose from PM: one toward IPL, concerning the action goal and one toward DCI concerning action vitality forms. This last finding opens an interesting question concerning the possibility to elicit VF in two distinct ways: cognitively (from PM to DCI) and affectively (from DCI to PM).

vitality forms | dynamic causal modeling | insula | parieto-frontal network | mirror neurons

In both monkeys and humans, there is a well-defined cortical network that becomes active during the execution, as well as during observation, of goal-directed motor acts (1–6), for example, grasping or reaching an object (7). This network includes areas of the inferior parietal lobe (IPL) and the premotor cortex (PM). In addition, areas of the posterior superior temporal sulcus (pSTS) become active predominantly during hand action observation indicating that this area is involved in the recognition of observed actions and that can forward information to the parieto-frontal network (8). It is important to note that the parieto-frontal network encodes the action content (i.e., the action goal) but does not appear to mediate the other fundamental aspect of actions: the action form (or vitality forms), i.e., how the action is performed. It should be stressed here that, regardless of their goal, all actions can be executed in different ways, e.g., gently or rudely. These forms of actions have been named vitality forms (VF) by Stern (9).

In the last years, several fMRI studies have shown that the observation of actions endowed with VF produces, in addition to the activation of the parieto-frontal network, activation of the dorso-central insula (DCI) (10–12). Notably, DCI is also activated during the execution of actions conveying VF, highlighting that this insular sector is endowed with the mirror mechanism.

According to Kurth et al. (13), the insula can be divided into four main functional domains: the sensorimotor domain which basically corresponds to the DCI, socioemotional, olfactory/gustatory, and cognitive domains. Most importantly, the insula receives inputs from different parts of the body conveying visceral, nociceptive, and somatosensory information. Given this input organization, the insula is thought to evince a representation of the body's internal state that, accordingly, modulates motor behavior (14). This proposal is supported by data concerning the anatomical connections of DCI with brain regions involved in the action observation–execution network. Specifically, monkey studies showed that the central sector of the insula is connected to the two main nodes of the classical parieto-frontal circuit: the rostral IPL area and the premotor area F5 (6, 15).

## Significance

During social interactions, people perform actions in different ways communicating their attitudes toward others. These aspects of action, named vitality forms (VF), are encoded in the dorso-central insula (DCI). Here, using dynamic causal modeling, we establish the direction of information flow between the insula and the parieto-frontal network, during the processing of actions endowed with (and without) VF. Results showed that, during action observation, two streams arose from pSTS: one toward IPL (action goal) and one toward DCI (action VF). During action execution, two streams arose from premotor cortex (PM): one toward IPL (goal) and one toward DCI (VF). This finding rises a question regarding the possibility to elicit VF in two distinct ways: cognitively (via PM) or affectively (via DCI).

Author contributions: G.D.C. and P.Z. designed research; G.D.C. performed research; G.D.C., G.L., and B.A.U. analyzed data; A.S. contributed with material and consulting for the development of the project; and G.D.C., A.S., K.J.F., and G.R. wrote the paper.

Reviewers: R.G., Universiteit Maastricht; F.S., Università degli Studi di Padova; and M.T., Università di Milano Bicocca.

The authors declare no competing interest.

Copyright © 2024 the Author(s). Published by PNAS. This article is distributed under [Creative Commons Attribution-NonCommercial-NoDerivatives License 4.0 \(CC BY-NC-ND\)](https://creativecommons.org/licenses/by-nc-nd/4.0/).

<sup>1</sup>To whom correspondence may be addressed. Email: giacomo.rizzolatti@unipr.it.

This article contains supporting information online at <https://www.pnas.org/lookup/suppl/doi:10.1073/pnas.2402282121/-/DCSupplemental>.

Published June 17, 2024.

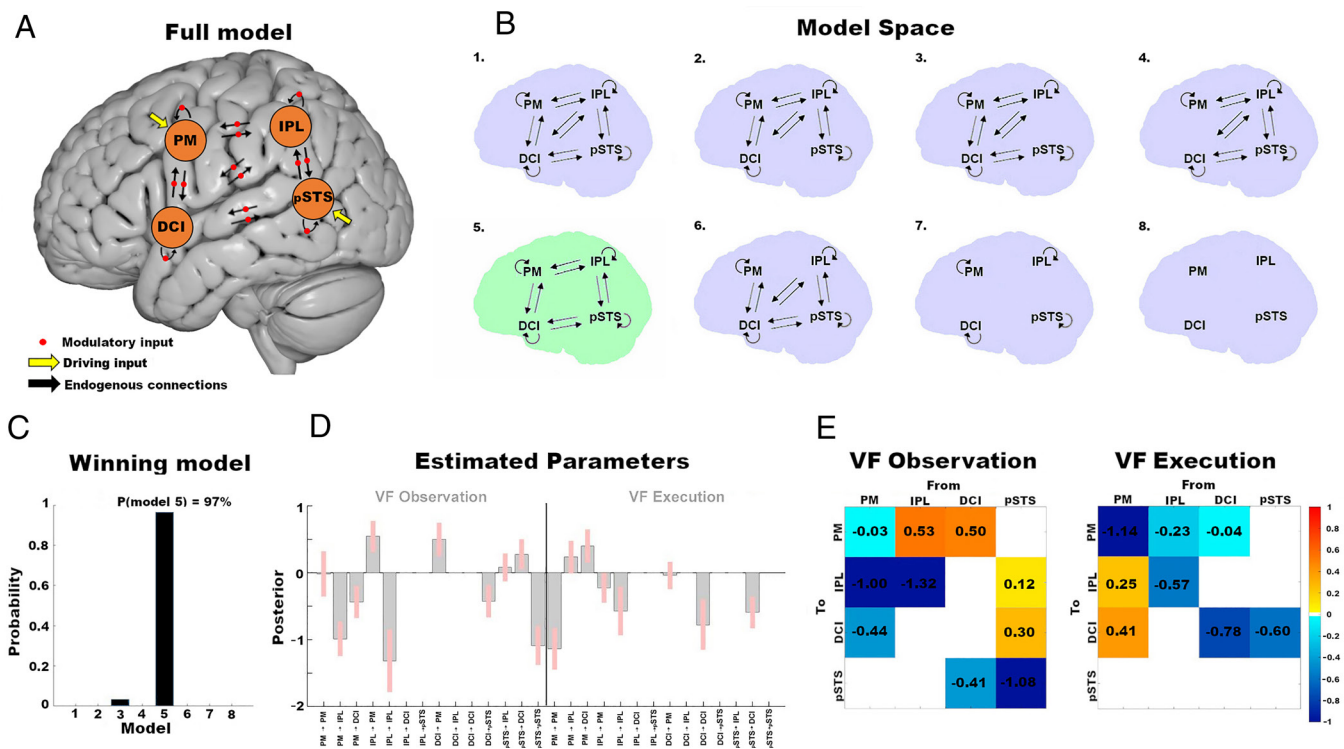


**Fig. 1.** The “full” DCM structure (A). Black arrows represent average connectivity (A matrix). Yellow arrows represent driving inputs entering in PM (EXE) and pSTS (OBS). Red dots represent modulatory inputs VF EXE and VF OBS (B matrix) which were enabled to modulate all connections, including self-inhibitory connections (curved black arrows). Model space including the full model (1), six reduced models (2 to 7)—in which we switched off the modulatory inputs entering in specific connections—and a “null” model (8) with no modulation serving as baseline (B). The best model was model 5 (connections between DCI and IPL are not modulated by VF) with a posterior probability of 97% (C). BMA of the model parameters which survived a thresholding at posterior probability >95%. Each parameter on the x axis refers to the modulation effect of a condition (VF Observation and VF Execution) on each specific connection (D). Effective connectivity matrices (E). For off-diagonal values, changes in connectivity strengths are represented in a scale from yellow to red, if excitatory, and from turquoise to blue, if inhibitory. For leading diagonal values, representative of self-connectivity, which is inhibitory by definition, the color code is inverted (more positive values correspond to more self-inhibition, more negative values correspond to disinhibition, compared to the default of  $-0.5$  Hz).

In humans, DCI appears to correspond to the portion of the macaque insula that is connected with the parieto-frontal network (16). Its electrical stimulation elicits hand movements (17). A probabilistic tractography study—of both humans and monkeys—confirmed these findings, showing that DCI is anatomically connected with the parieto-frontal circuit involved in the control of reaching/grasping movements (18). Furthermore, the connection between DCI and STS region in humans was assessed by Almashaiki and colleagues, showing that the stimulation of DCI activated areas of the STS region (19). These results are in line with the findings of Ghaziri et al. who demonstrated, in humans, a functional connectivity between DCI and STS (20).

Given these findings, a next fundamental step is to establish the causal role played by DCI in relation to the parieto-frontal network, during the execution and observation of actions endowed with VF. To this purpose, in the present study, we assessed the direction of information flow across four cortical nodes: DCI, pSTS, the border between PMv/PMd (together referred as PM) and IPL, to establish the interaction of these cortical nodes in execution and observation of action VF. Using dynamic causal modeling (DCM) (21–24), we analyzed data from an fMRI study employing a classical VF paradigm in which participants have been asked: 1) to observe a hand/arm action (observation task, OBS); 2) to execute the same observed action (execution task, EXE). Specifically, in the OBS task, participants observed video clips showing an actor performing a passing action with his right arm, performed gently or rudely toward another actor (vitality form condition), or without any VF, i.e., actions performed with constant velocity (control condition). In the EXE task, according to the instruction, participants were

required to move an object located on a plane, as if offering it to another person, gently and rudely (vitality form condition), or move it without any VF (control condition).

The results of the Bayesian model comparison showed that, during action observation, pSTS, a high-order visual area, gives origin to two streams, one toward IPL for the action goal encoding, and one toward DCI for the encoding of action vitality form. During action execution, motor information derives from PM and also gives origin to two streams: one, related to the action goal toward IPL, and one concerning the action vitality form toward DCI. This last finding appears to suggest that PM contains a repertoire of actions tagged with specific VF. It also opens an interesting question regarding the possibility to elicit VF in two distinct ways: cognitively (from PM to DCI) or affectively (with a modulation effect from DCI to PM).

## Results

Results of the parametric empirical Bayes (PEB) analysis showed that a particular architecture of directed connectivity (model 5) best explained our data, with a posterior probability of 97%, in relation to alternative plausible architectures (Fig. 1 B and C). This model precluded connections between DCI and IPL from showing a modulatory effect of VF during both the observation and execution tasks. By thresholding the Bayesian model average (BMA) of directed connectivity estimates at >95% posterior probability (based on the free energy approximation to the evidence for models with and without connectivity changes), we identified the connections (i.e., model parameters) that were modulated by

## Action Observation Network

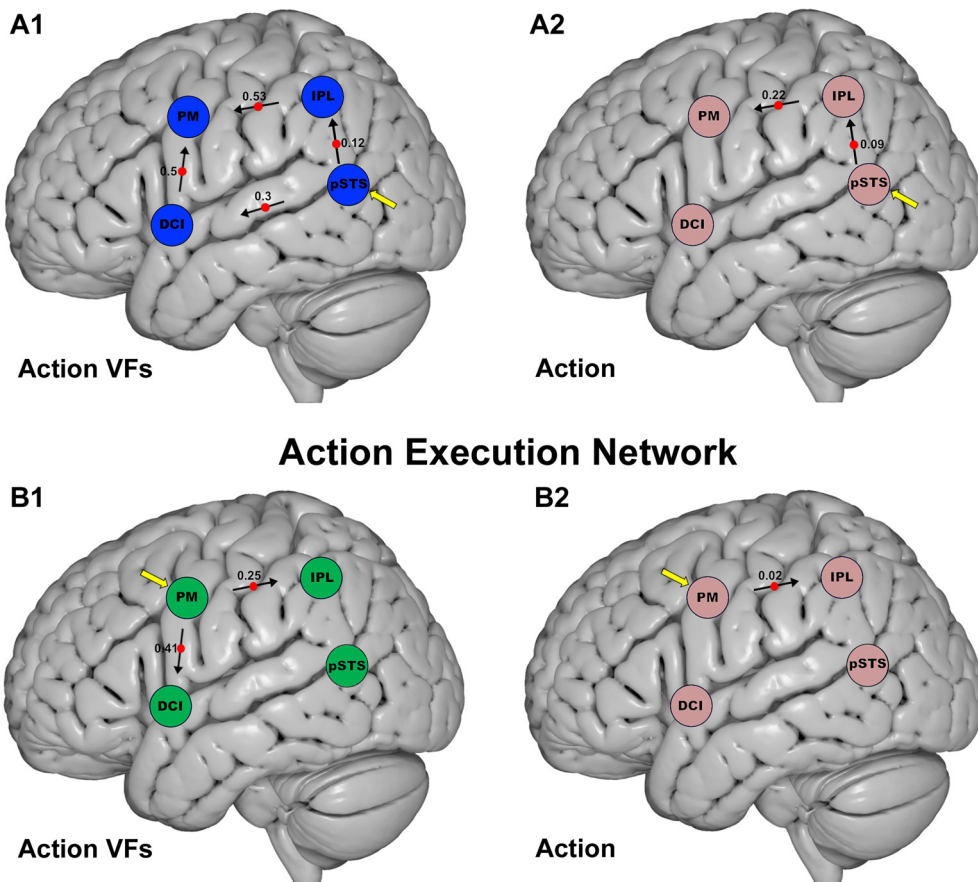


**Fig. 2.** Modulatory connection strengths in the winning models relative to the OBS and EXE tasks surviving at BMA thresholding at >95% posterior probability (strong evidence). Red dots represent positive modulation effects during the VF observation (A1), control observation (A2), VF execution (B1), and control execution (B2). Yellow arrows indicate driving inputs where the visual and motor information of action start.

VF (Fig. 1D). These parameters are also shown in Fig. 1E as connectivity matrices, in which a positive sign (yellow and orange squares) represents a positive modulation while a negative sign (turquoise and blue squares) represents a negative modulation. Self-connections (diagonal) are inhibitory by construction: positive self-connections represent more inhibition and negative self-connections represent disinhibition (21, 22).

Considering extrinsic (between-region) connectivity during the VF observation task, results revealed a positive modulation—i.e., increase—of the connections from pSTS to IPL (0.12), from IPL to PM (0.53), from pSTS to DCI (0.3), and from DCI to PM (0.5) (Fig. 2A1). During the VF, results revealed an increase in the directed connections from PM to IPL (0.25) and from PM to DCI (0.41) (Fig. 2B1). Additionally, results showed a strong “disinhibition effect” via the self-connections of IPL (−1.32) and pSTS (−1.08) during the observation of vitality forms (Fig. 1 E, Left panel) and of PM (−1.14), IPL (−0.57), and DCI (−0.78) during the execution of vitality forms (Fig. 1 E, Right panel). Above, changes in connectivity are expressed in terms of relative log scaling (with adimensional units), such that a positive change reflects an increase, and a negative change reflects a decrease.

Notably, these findings were also supported by an exhaustive (greedy or automatic) search of all models with and without VF effects on each connection. This analysis revealed similar changes in connectivity among the nodes considered (SI Appendix, Fig. S2). Particularly, the automatic search showed a positive modulation (thresholding at 95% posterior probability) of the

connections from IPL to PM (0.56), from DCI to PM (0.48), and a disinhibition effect of IPL (−1.40) and pSTS (−0.99) during the observation of VF. In addition, this approach showed a positive modulation (thresholding at 95% posterior probability) of the connections from PM to DCI (0.36) and a disinhibition effect of PM (−1.05), IPL (−0.69), and DCI (−0.82) during the execution of VF (SI Appendix, Fig. S2A). Finally, to verify the specificity of the winning model 5—in accounting for the processing of VF during the observation and execution tasks—we tested how the information flow between its nodes was modulated by the control conditions, comprising the observation (CT OBS) and execution (CT EXE) of neutral actions performed with constant velocity.

Results after BMA thresholding (at >95% posterior probability) revealed that during the observation of neutral actions, there was a positive modulation from pSTS to IPL (0.09) and from IPL to PM (0.22) (Fig. 2A2). In addition, during the execution of control actions, there was a positive modulation from PM to IPL (0.02) (Fig. 2B2) and a negative modulation from PM to DCI (−0.13) (see also SI Appendix, Fig. S2B). Connectivity parameters involving the DCI did not survive the BMA thresholding, suggesting the specific involvement of DCI only during the processing of VF.

## Discussion

The neural basis of goal-directed motor actions consists of a cortical network comprising parietal and frontal areas (1–6). This same network is active not only during the execution of goal-directed

motor actions but also during the observation of the same actions (1). In addition to the goal, another fundamental feature of an action is the manner in which it is carried out, i.e., its form. When we interact with others, the same motor act may be performed with different VF (gentle, neutral, enthusiastic, rude, etc.) (see also ref. 25). For example, when we meet a person, we can greet this person warmly or coldly, the form reflecting whether we are happy to meet him or whether our gesture is a merely greeting of circumstance. Similarly, the observation of the action VF performed by others allows us to understand their positive or negative dispositions toward the person in question. In the last years, several fMRI studies have provided evidence that both the observation and the execution of actions expressed with VF produce, in addition to the activation of the parieto-frontal network, the activation of the DCI (10, 11) and in some studies of the middle cingulate cortex (MCC) (12). These findings suggest that, while the parieto-frontal network is responsible for the action goal processing, the DCI, and in some cases also MCC, are the areas involved in the processing of action VF.

In the present study, we used DCM (21, 22) to quantify the directed information flow when processing action goals and VF, respectively. For this purpose, we carried out an fMRI study employing a classical VF paradigm in which participants were asked: 1) to observe a hand/arm action (observation task); 2) to execute the same action (execution task). In this study, actions were either executed with a specific vitality form (gentle or rude) or were performed in a neutral way, i.e., to minimize, or possibly to eliminate, the presence of vitality forms. After conducting standard fMRI analysis, we selected four cortical nodes known to be involved in arm/hand goal-directed actions. These nodes corresponded to the following cortical regions: pSTS, IPL, PM, and DCI.

Results show that the observation of actions endowed with VF activates the higher-order visual areas around the posterior part of the superior temporal sulcus (pSTS). Two streams originate from this region: the first reaches IPL and then PM, i.e., the areas forming the classical network involved in the action goal understanding, while the second stream, leaving the visual areas, reaches DCI and then PM. The demonstration of this last network supports the view that the stream connecting DCI-PM underlies the action form recognition. It is important to note that, during the observation of actions without an affective content, i.e., a vitality form, there is no activation of this stream, thus foregrounding its specific involvement in the processing of action VF.

Results relative to the execution of action endowed with VF show, first, an initial activation of PM. From this motor area, two streams originate. One reaches IPL, a region known to be involved, alongside with the premotor motor areas, in the execution of goal-directed actions (26), while the other reaches DCI. This VF effect on connectivity was unexpected because it is generally assumed that, when an action is executed with a specific VF, it is DCI that modulates the parieto-frontal network on the basis of the internal affective state of the agent. The finding that—during the execution of action VF—PM modulates DCI, rather than the other way around, deserves some discussion.

Specifically, in our fMRI study, during the action execution task, participants had to voluntarily perform the correct action VF, after reading the color of the edge screen (blue color: gentle action; red color: rude action). It is rather unlikely that after reading an instruction, they could immediately enter into the specific instructed affective state. Rather, it is more likely that they performed the action with the instructed vitality form using a cognitive command, most probably prefrontal, instead of actually

entering into the instructed affective state. This action selection is performed regardless of the affective state of the agent. The subsequent activation of DCI possibly furnishes an affective information for the executed action. These considerations suggest that in PM, there is a “repertoire” of kinematically distinct motor acts that may be selected according to the intention on how to behave (e.g., positively or negatively), regardless of the affective state of the agent.

The modulation effect of PM on DCI opens an important perspective regarding the execution of action VF. It appears that VF could have a “cognitive” and an “affective” origin. When VF are cognitively planned, it might involve the activation of the frontal lobe and subsequently activate PM and then DCI. In this view, when the agent voluntarily decides to perform an action VF, the parieto-frontal circuit modulates the DCI. In this way, the motor action acquires an affective component. In contrast, when VF convey a real positive or negative affective state, they might originate in DCI and possibly, in some subcortical structures, and modulate the parieto-frontal circuit selecting the appropriate motor act encoded in PM area. For example, if an individual feels enthusiastic toward a friend, this attitude will positively modulate his motor behavior and consequently the action will be performed with a positive VF. In this view, a motor act acquires the positive affective aspect.

As with all DCM studies, our conclusions rest upon assessing the evidence for different models or hypotheses. The requisite Bayesian model comparison depends upon the models specified. This means that the model with the greatest evidence is not necessarily the best (or true) model: it is simply the best explanation among the hypotheses considered. The particular set of hypotheses evaluated in this work addressed the direction of information flow—during observation and execution of actions—and its context sensitivity. We therefore used a minimally complex subnetwork or subgraph within which to test for condition-specific effects on directed connectivity. Clearly, different questions would call for a different set of models: e.g., questions asking whether the driving input (for execution) is limited to PM or distributed over several regions.

The activation of PM during the processing of actions may be related to its encoding of the physical properties of actions (27). This is in line with results of Di Dio et al. (7) demonstrating that, in humans, the premotor and parietal areas are involved in the encoding of reaching movements performed with biological motion. Furthermore, Di Dio et al. demonstrated that the observation of different velocities produced an increase of parieto-frontal network activity indicating its specific involvement in the velocity processing. Moreover, Casile et al. (28) demonstrated that the observation of movements complying with human kinematic laws of motion produced the activation of the dorsal premotor cortex (PMd) extending to the ventral sector (PMv).

Pooling together, our findings clearly indicate that, during the observation and execution of goal-directed actions, two streams arise from visual and motor areas: a dorsal stream encoding the action goal and a ventral stream encoding the action VF. While the processing of visual information of VF during action observation was in line with the hypothesis proposed in our previous work (11), the modulation effect of PM toward DCI during the execution of VF was unexpected.

These findings open a further question regarding the possibility to elicit VF in two distinct ways: cognitively or affectively. While in the present study, we investigated VF triggered by a cognitive command given by the experiment, future experiments are needed to investigate affective VF conveying a real internal state.

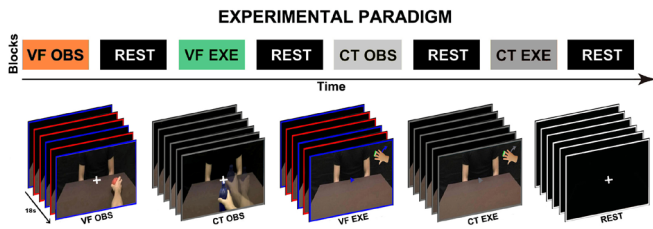


**Fig. 3.** Experimental Paradigm. In the observation task, participants were asked either to observe actions conveying VF (VF OBS) or to observe the same actions performed with constant velocity (control condition, CT OBS). In the execution task (VF EXE), participants were asked to perform the action gently (blue color), rudely (red color), or neutrally (CT EXE). Between blocks, an interblock interval lasting 18 s was presented (Rest).

## Methods

**Participants.** Twenty-two healthy right-handed volunteers (12 females and 10 males, mean age = 22.7, SD = 2.4) took part in the fMRI experiment. All participants had normal or corrected-to-normal visual acuity. None of them reported a history of psychiatric or neurological disorders or current use of any psychoactive medications. They gave their written informed consent to be subjected to the experimental procedure, which was approved by the Local Ethics Committee of Parma (552/2020/SPER/UNIPR) in accordance with the Declaration of Helsinki. The data from all participants were subject to DCM.

**Paradigm and Task.** The fMRI experiment comprised three functional runs. In each run, participants were presented with videos regarding two tasks (OBS and EXE) and two different conditions (vitality forms, VF; control, CT). In total, four conditions were presented in independent miniblocks (VF OBS, VF EXE, CT OBS, CT EXE) in a randomized order (see also SI). The OBS task started with the instruction to “observe the action” and required the participants to focus on the action performed with VF (VF OBS) or without VF (CT OBS). Specifically, during the VF condition, participants observed actions performed in first person perspective with gentle or rude VF (VF OBS; Fig. 3). During the control condition, participants observed the same actions performed with constant velocity (CT OBS; Fig. 3). The aim of the control stimuli was to allow participants to understand the action goal without conveying any vitality form information.

The EXE task started with the instruction “perform the action” and required the participants to execute the action themselves. During the EXE task, participants were presented with a static image of an actor seated opposite to them and were

asked to move a little box toward the actor with different vitality forms (VF EXE) or without vitality forms (CT EXE), by simply rotating the wrist. A cue presented in the center of the screen indicated the start of the action. The color of the screen edge indicated the vitality form observed during the OBS task or the vitality form with which the action had to be executed during the EXE task (blue color: gentle; red color: rude; gray color: neutral, Fig. 3). In both OBS and EXE tasks, in each video, a fixation cross was introduced to control for restrained eye movements (see also *SI Appendix, Extended Methods*).

**fMRI Data Acquisition and Analysis.** Anatomical T1-weighted and functional T2\*-weighted MR images were acquired with a 3 Tesla General Electrics scanner (see details in *SI Appendix*). After standard preprocessing steps, data were analyzed using a random-effects model, implemented in a two-level procedure. In the first level, the fMRI BOLD signal of each participant was modeled using a general linear model (GLM), with a design-matrix comprising the onsets, the durations of each event according to the experimental task for each functional run. The GLM comprised the following regressors: Vitality forms Observation (VF OBS), Control Observation (CT OBS), Vitality forms Execution (VF EXE), Control Execution (CT EXE), and Instruction. Within each block, the videos were modeled as a whole event lasting 18 s. The instruction was modeled with a duration of 3 s. In the second-level analysis (group-analysis), corresponding contrast images of the first level for each participant were entered into a flexible ANOVA with sphericity-correction for repeated measures. This model was composed of four regressors (VF OBS, CT OBS, VF EXE, and CT EXE) and considered the activation pattern obtained for different tasks (OBS and EXE) in two different conditions (vitality forms and control). Within this model, we assessed activations associated with each task versus implicit baseline (fixation cross). To identify the overall activity patterns involved in both the observation and execution of VF, a conjunction analysis (conjunction null) was carried out (OBS VF & EXE VF, see also *SI Appendix, Fig. S1*). After the identification of this activity pattern, the following four regions or nodes were identified: pSTS, IPL, PM, and DCI (Fig. 4).

## DCM.

**Theoretical background.** DCM is an analysis framework for identifying models of effective connectivity, i.e., the directed causal influence among brain regions (21). In the DCM framework, the rate of change of neural activity of each brain region at a specific point in time ( $\dot{z}$ ) can be expressed as a function of the experimental inputs ( $u$ ) and the connectivity between and within brain regions. This is approximated by a neuronal state equation:

## ACTION OBSERVATION AND EXECUTION NETWORK

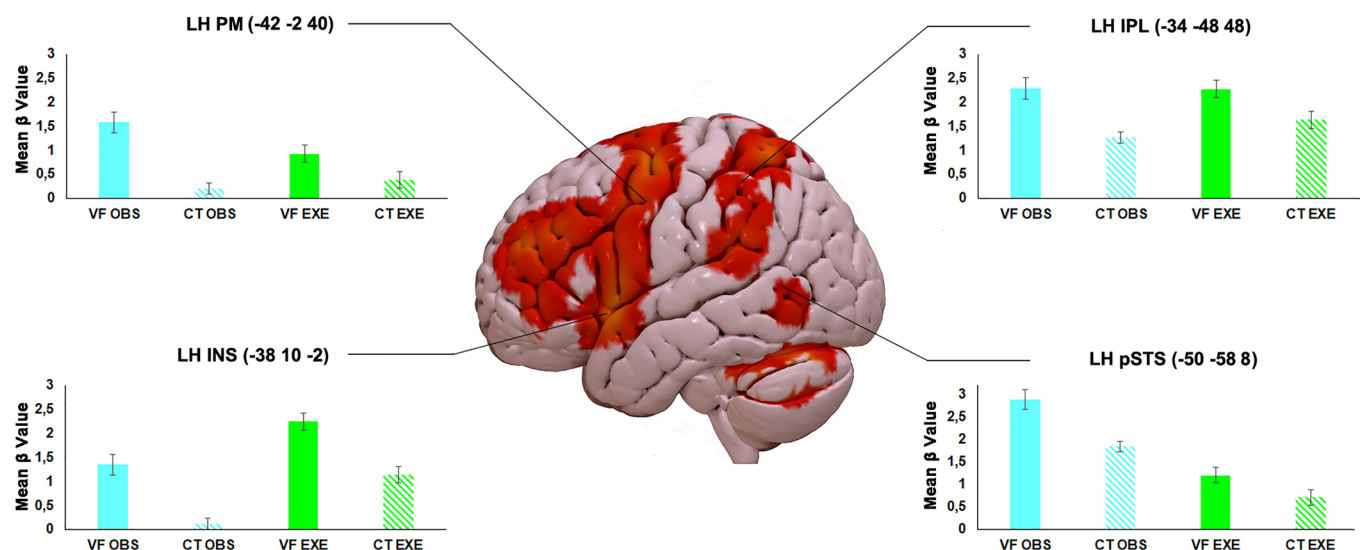


**Fig. 4.** Brain activations resulting from the “conjunction null” analysis between VF observation and VF execution. This activation map was used to identify and select the nodes for DCM analysis. These activations are rendered onto a standard MNI brain template (pFWE < 0.05 at cluster level).

$$\dot{z} = (A + \sum_{j=1}^m u_j B^{(j)})z + Cu.$$

The experimental inputs can enter the model by eliciting direct influences on specific regions at the onset of each stimulus (*driving* inputs) or they can modulate the connections among brain regions (*modulatory* inputs). The parameter matrices A, B, and C describe three kinds of connectivity, which underlie the modeled neural dynamics: the A-matrix represents the intrinsic or average (baseline) connectivity within the network of brain regions; the B-matrix represents changes in effective connectivity due to the modulatory inputs; and the C-matrix represents the rate of change of the neural response due to the driving inputs. Additionally, each brain region is equipped with an inhibitory self-connection which represents its gain or sensitivity to inputs. From a biological point of view, self-connections control the excitatory-inhibitory balance, mediated by the interaction of pyramidal cells and inhibitory interneurons (29). **VOI selection and time-series extraction.** The first step of DCM analysis entailed the identification of regions of interest and corresponding time-series extraction. In the present study, we selected four nodes involved in both observation and execution of actions conveying VF: pSTS, IPL, PM, and DCI. Four spheric ROIs were created for each participant around the coordinates identified at the group level [(pSTS:  $-50 -58 8$  (mean:  $-50 -58.18 7.1$ , SD:  $0 1.05 0.58$ ; IPL:  $-34 -48 48$  (mean:  $-34 -47.64 48.18$ , SD:  $0 1.002 0.85$ ; PM  $-42 -2 40$  (mean:  $-42.18 -1.8 39$ , SD:  $0 1.43 1.82$ ); DCI:  $-38 10 -2$  (mean:  $-38 10 -1.5$ , SD:  $0 0.62 1.53$ )]. When a subject did not show activation at one of these specific coordinates, we relaxed the *P*-value (until  $P < 0.05$ ) to find activated voxels at or close to the expected location. Finally, for each ROI, the time series data regarding four different conditions were extracted (OBS\_VF, OBS\_CT, EXE\_VF, EXE\_CT) by using the principal eigenvariate of all voxels within a sphere of 5 mm radius.

**First-level DCM analysis.** The second step of the DCM analysis involved the specification of a full model for each participant (Fig. 1A). In this model, matrix A modeled recurrent connections between all four regions of interest (except for the connection between PM and pSTS) and inhibitory self-connections for each region. From the GLM regressors, we define OBS (observation) as driving input entering in pSTS and EXE (execution) as driving input entering in PM. Concerning the execution task, we switched off pSTS because participants performed actions without seeing their hand. To test the effect of vitality forms on the effective connectivity of the circuit (both during observation and execution), the GLM regressors VF OBS and VF EXE were used as modulatory inputs and were allowed to modulate all connections, including self-inhibitory ones.

**Second-level DCM analysis with PEB.** After the estimation of each subject's full DCM, we took the estimated connectivity parameters from each full model to the group level and ran a PEB analysis (second-level analysis). The PEB analysis captures the commonalities and differences between participants and returns

a score (Free energy: F) for the quality of the group-level model (22). This free energy score, also called the evidence lower bound (ELBO) in machine learning, quantifies the trade-off between the accuracy and complexity of the model, where more positive values are better. By comparing the free energies resulting from different PEB models, with different set of parameters switched on and off, one can select the model with the greatest free energy or model evidence and thereby find the best explanation for the dataset. In the present study, we were interested in identifying the best explanation for the commonalities across our subjects in terms of changes in effective connectivity due to a modulatory effect of vitality forms during action observation and execution.

Starting from the full model, we defined a model space containing reduced models with different configurations of the B-matrix. Specifically, in each reduced model, the modulation effect of vitality form entering the connection between two regions was switched off. In total, the model space contained eight candidate models: a full model, six reduced models, and a null model with no modulation to serve as a baseline (Fig. 1B). Bayesian model comparison (*spm\_dcm\_peb\_bmc* function) was used to assess the evidence for each model. In addition, in order to summarize parameters across all models and obtain numerical estimates for each of them, a BMA was computed (30, 31). Finally, to validate and strengthen the results suggested by the analysis based on prespecified reduced models, we used an automatic search approach over all (modulatory) connection parameters. This procedure automatically prunes away any parameters which do not contribute to the model evidence. The result is a BMA over the 256 most probable models, weighted by their evidence (*SI Appendix, Fig. S2*).

**Data, Materials, and Software Availability.** The DCM Dataset have been deposited in Zenodo (<https://zenodo.org/records/11202536>).

**ACKNOWLEDGMENTS.** This work has been supported by the following: 1) Starting Grant from the European Research Council under the European Union's Horizon 2020 research and innovation program (G.A. No 804388, wHiSPER); 2) National Recovery and Resilience Plan, Mission 4 Component 2 Investment 1.2-Call for tender No. 247 of 19/08/2022 and No. 367 of 07/10/2022 of Italian Ministry of University and Research funded by the European Union-NextGenerationEU (Project code SOE\_0000049). 3) This research was funded in part by the Wellcome Trust [203147/Z/16/Z].

Author affiliations: <sup>a</sup>Department of Medicine and Surgery, University of Parma, Parma 43125, Italy; <sup>b</sup>Cognitive Architecture for Collaborative Technologies Unit, Italian Institute of Technology, Genova 16163, Italy; <sup>c</sup>Department of Informatics, Bioengineering, Robotics and Systems Engineering, University of Genoa, Genoa 16145, Italy; <sup>d</sup>Wellcome Centre for Human Neuroimaging, Institute of Neurology, University College London, London WC1N 3BG, United Kingdom; <sup>e</sup>Department of Psychology, Bilkent University, Ankara 06800, Turkey; <sup>f</sup>Department of Neuroscience, Bilkent University, Ankara 06800, Turkey; <sup>g</sup>Aysel Sabuncu Brain Research Center & National Magnetic Resonance Research Center, Bilkent University, Ankara 06800, Turkey; and <sup>h</sup>Institute of Neuroscience, National Research Council of Italy, Parma 43125, Italy

1. G. Rizzolatti, C. Sinigaglia, The mirror mechanism: A basic principle of brain function. *Nat. Rev. Neurosci.* **17**, 757–765 (2016), 10.1038/nrn.2016.135.
2. G. Rizzolatti, L. Fadiga, V. Gallese, L. Fogassi, Premotor cortex and the recognition of motor actions. *Brain Res. Cogn. Brain Res.* **3**, 131–141 (1996), 10.1016/0926-6410(95)00038-0.
3. S. Rozzi, P. F. Ferrari, L. Bonini, G. Rizzolatti, L. Fogassi, Functional organization of inferior parietal lobule convexity in the macaque monkey: Electrophysiological characterization of motor, sensory and mirror responses and their correlation with cytoarchitectonic areas. *Eur. J. Neurosci.* **28**, 1569–1588 (2008), 10.1111/j.1460-9568.2008.06395.x.
4. G. Rizzolatti, G. Luppino, The cortical motor system. *Neuron* **31**, 889–901 (2001), 10.1016/S0896-6273(01)00423-8.
5. G. Rizzolatti, L. Craighero, The mirror-neuron system. *Ann. Rev. Neurosci.* **27**, 169–192 (2004), 10.1146/annurev.neuro.27.070203.144230.
6. S. Bruni *et al.*, Cortical and subcortical connections of parietal and premotor nodes of the monkey hand mirror neuron network. *Brain Struct. Funct.* **223**, 1713–1729 (2018), 10.1007/s00429-017-1582-0.
7. G. Di Dio *et al.*, The neural correlates of velocity processing during the observation of a biological effector in the parietal and premotor cortex. *Neuroimage* **1**, 425–436 (2013), 10.1016/j.neuroimage.2012.09.026.
8. G. Rizzolatti, L. Fogassi, The mirror mechanism: Recent findings and perspectives. *Philos. Trans. R Soc. London B, Biol. Sci.* **369**, 20130420 (2014), 10.1098/rstb.2013.0420.
9. D. N. Stern, *The Interpersonal World of the Infant* (New York Basic Book, 1985).
10. G. Di Cesare, C. Di Dio, M. Marchi, G. Rizzolatti, Expressing our internal states and understanding those of others. *Proc. Natl. Acad. Sci. U.S.A.* **112**, 10331–10335 (2015), 10.1073/pnas.1512133112.
11. G. Di Cesare, M. Gerbella, G. Rizzolatti, The neural bases of vitality forms. *Natl. Sci. Rev.* **7**, 202–213 (2020), 10.1093/nsr/nwz187.
12. G. Di Cesare *et al.*, The middle cingulate cortex and dorso-central insula: A mirror circuit encoding observation and execution of vitality forms. *Proc. Natl. Acad. Sci. U.S.A.* **118**, e2111358118 (2021), 10.1073/pnas.2111358118.
13. F. Kurth, K. Zilles, P. T. Fox, A. R. Laird, S. B. Eickhoff, A link between the systems: Functional differentiation and integration within the human insula revealed by meta-analysis. *Brain Struct. Funct.* **214**, 519–534 (2010), 10.1007/s00429-010-0255-z.
14. A. D. Craig, How do you feel? Interoception: The sense of the physiological condition of the body. *Nat. Rev. Neurosci.* **3**, 655–666 (2002), 10.1038/nrn894.
15. M. Gerbella, E. Borra, S. Tonelli, S. Rozzi, G. Luppino, Connectional heterogeneity of the ventral part of the macaque area 46. *Cereb. Cortex* **23**, 967–987 (2013), 10.1093/cercor/bhs096.
16. A. Jezzini *et al.*, A shared neural network for emotional expression and perception: An anatomical study in the macaque monkey. *Front. Behav. Neurosci.* **9**, 1–17 (2015), 10.3389/fnbeh.2015.00243.
17. A. Jezzini, F. Caruana, I. Stoianov, V. Gallese, G. Rizzolatti, Functional organization of the insula and inner perisylvian regions. *Proc. Natl. Acad. Sci. U.S.A.* **109**, 10077–10082 (2012).
18. G. Di Cesare *et al.*, Insula connections with the parieto-frontal circuit for generating arm actions in humans and macaque monkeys. *Cereb. Cortex* **29**, 2140–2147 (2019).
19. T. Almashaikhi *et al.*, Functional connectivity of insular efferences. *Hum. Brain Mapp.* **35**, 5279–5294 (2014), 10.1002/hbm.22549.
20. J. Ghaziri *et al.*, The corticocortical structural connectivity of the human insula. *Cereb. Cortex* **27**, 1216–1228 (2017), 10.1093/cercor/bhw308.
21. P. Zeidman *et al.*, A guide to group effective connectivity analysis, part 1: First level analysis with DCM for fMRI. *Neuroimage* **15**, 174–190 (2019), 10.1016/j.neuroimage.2019.06.031.
22. P. Zeidman *et al.*, A guide to group effective connectivity analysis, part 2: Second level analysis with PEB. *Neuroimage* **15**, 12–25 (2019), 10.1016/j.neuroimage.2019.06.032.
23. K. J. Friston, L. Harrison, W. Penny, Dynamic causal modelling. *Neuroimage* **19**, 1273–1302 (2003).

24. W. D. Penny, K. E. Stephan, A. Mechelli, K. J. Friston, Modelling functional integration: A comparison of structural equation and dynamic causal models. *Neuroimage* **23**, S264-S274 (2004).
25. L. Lastrico *et al.*, "Expressing and inferring action carefulness in human-to-robot handovers" in *2023 IEEE/RSJ International Conference on Intelligent Robots and Systems (IROS)*, (Detroit, MI, 2023), pp. 9824-9831.
26. S. Rozzi *et al.*, Cortical connections of the inferior parietal cortical convexity of the macaque monkey. *Cereb. Cortex* **16**, 1389-1417 (2006), 10.1093/cercor/bhj076.
27. F. Filimon, J. D. Nelson, D. J. Hagler, M. I. Sereno, Human cortical representations for reaching: Mirror neurons for execution, observation, and imagery. *NeuroImage* **37**, 1315-1328 (2007), 10.1016/j.neuroimage.2007.06.008.
28. A. Casile *et al.*, Neuronal encoding of human kinematic invariants during action observation. *Cereb. Cortex* **20**, 1647-1655 (2010), 10.1093/cercor/bhp229.
29. R. N. Bastos, X. Penate, M. Bates, D. Hammond, F. A. Barr, CYK4 inhibits Rac1-dependent PAK1 and ARHGEF7 effector pathways during cytokinesis. *J. Cell Biol.* **198**, 865-880 (2012).
30. J. A. Hoeting, D. Madigan, A. E. Raftery, C. T. Volinsky, Bayesian model averaging: A tutorial (with comments by M. Clyde, David Draper and El George, and a rejoinder by the authors. *Stat. Sci.* **14**, 382-417 (1999).
31. W. Penny, G. Flandin, N. Trujillo-Barreto, Bayesian comparison of spatially regularised general linear models. *Hum. Brain Mapp.* **28**, 275-293 (2007), 10.1002/hbm.20327.